Physics and Imaging in Radiation Oncology 18 (2021) 1–4

Contents lists available at ScienceDirect

Physics and Imaging in Radiation Oncology

journal homepage: www.sciencedirect.com/journal/physics-and-imaging-in-radiation-oncology

Visualizing the urethra by magnetic resonance imaging without usage of a catheter for radiotherapy of prostate cancer

Takaaki Yoshimura [a,b], Kentaro Nishioka [c], Takayuki Hashimoto [c], Taro Fujiwara [d], Kinya Ishizaka [d], Hiroyuki Sugimori [e], Shoki Kogame [f], Kazuya Seki [f], Hiroshi Tamura [d], Sodai Tanaka [b,g], Yuto Matsuo [b], Yasuhiro Dekura [h], Fumi Kato [i], Hidefumi Aoyama [h], Shinichi Shimizu [b,c,j,*]

[a] Department of Health Sciences and Technology, Faculty of Health Sciences, Hokkaido University, Sapporo, Japan
[b] Department of Medical Physics, Hokkaido University Hospital, Sapporo, Japan
[c] Department of Radiation Medical Science and Engineering, Faculty of Medicine, Hokkaido University, Sapporo, Japan
[d] Department of Radiation Technology, Hokkaido University Hospital, Sapporo, Japan
[e] Department of Biomedical Science and Engineering, Faculty of Health Sciences, Hokkaido University, Sapporo, Japan
[f] Division of Radiological Science and Technology, Department of Health Sciences, School of Medicine, Hokkaido University, Sapporo, Japan
[g] Faculty of Engineering, Hokkaido University, Sapporo, Japan
[h] Department of Radiation Oncology, Faculty of Medicine, Hokkaido University, Sapporo, Japan
[i] Department of Diagnostic and Interventional Radiology, Hokkaido University Hospital, Sapporo, Japan
[j] Global Center for Biomedical Science and Engineering, Faculty of Medicine, Hokkaido University, Sapporo, Japan

ARTICLE INFO

Keywords:
Urethra-sparing radiotherapy
Magnetic resonance imaging
Prostate cancer

ABSTRACT

The urethra position may shift due to the presence/absence of the catheter. Our proposed post-urination-magnetic resonance imaging (PU-MRI) technique is possible to identify the urethra without catheter. We aimed to verify the inter-operator difference in contouring the urethra by PU-MRI. The mean values of the evaluation indices of dice similarity coefficient, mean slice-wise Hausdorff distance, and center coordinates were 0.93, 0.17 mm, and 0.36 mm for computed tomography, and 0.75, 0.44 mm, and 1.00 mm for PU-MRI. Therefore, PU-MRI might be useful for identifying the prostatic urinary tract without using a urethral catheter.

Clinical trial registration: Hokkaido University Hospital for Clinical Research (018-0221).

1. Introduction

Prostate cancer is the most common disease in men and has multiple treatment options, including radiation therapy [1,2]. To increase the local control during radiation therapy, high-dose radiation is delivered uniformly to tumors [1–4]. Besides, acute or late gastrointestinal and genitourinary (GU) toxicities can be reduced using image-guided radiotherapy with either conventional or hypo fractional schedule. However, this is often accompanied by a local inflammatory reaction, which manifests clinically as GU toxicities, such as frequency, dysuria, and urethral stricture [5–8].

Although treatment-planning computed tomography (CT) provides anatomical information and electron density for dose calculation, and magnetic resonance imaging (MRI) provides clear anatomical information on soft tissues [9,10], it is difficult to accurately determine the urethra in the acquired images without using a urethral catheter or injecting contrast agents [11]. These procedures are invasive and may increase patient discomfort, the risk of infection, and risk of iatrogenic urethral strictures [12]. Besides, it is not practical to insert a urethral catheter into a patient daily. Therefore, previous methods used to identify the prostatic urinary tract with the use of a urethral catheter has potential problems, such as increased infection risk due to the indwelling urethral catheter [13] or anatomical uncertainty/reproducibility of the urethral structure depending on the presence/absence of the catheter [14]. In our previous report, we demonstrated that the urethral position with a Foley catheter is different from that with a thin and soft guide-wire in a significant proportion of patients [14].

Ideally, urethra-sparing radiation therapy requires the identification of the prostatic urinary tract without inserting a urethral catheter. Recently, MRI has attracted remarkable attention for visualization of the

* Corresponding author at: Department of Radiation Medical Science and Engineering, Faculty of Medicine, Hokkaido University, Sapporo, Japan.
E-mail address: sshing@med.hokudai.ac.jp (S. Shimizu).

https://doi.org/10.1016/j.phro.2021.03.002
Received 20 July 2020; Received in revised form 15 March 2021; Accepted 17 March 2021
Available online 26 March 2021

prostatic urinary tract in a non-invasive manner. Kataria et al. described an approach using gadolinium-enhanced T2-weighted MRI for delineating the prostatic urinary tract [15]. Zakian et al. also compared two T2-weighted MRI parameters for visualizing the prostatic urinary tract [16]. Rai et al. presented the micturating urethrography technique without using a urethral catheter or contrast agent [17]. In their method, urinating during imaging generated a high contrast due to the increase in signal intensity of the urethra. Their results suggested that sustained enhancement of the proximal urethra for over 1 min allowed for urethral contouring [17]. However, there were some problems to overcome, such as the attachment of instruments for recovering urine and psychological burden on patients.

We hypothesized that it is possible to contour the prostatic urinary tract without a urethral catheter by using high resolution T2-weighted post-urination MRI (PU-MRI). Based on a previous study, we set up a non-invasive method for identifying the prostatic urinary tract using PU-MRI to eliminate problems associated with invasiveness [17]. Therefore, we aimed to evaluate the inter-operator difference while contouring the prostatic urinary tract using PU-MRI and compared it with traditional visualization techniques that use a urethral catheter.

2. Materials and methods

2.1. Patient data

To evaluate the utility of urethral contouring, 11 patients with localized prostate cancer who had received spot scanning proton beam therapy in our institution from October 2019 to February 2020 were enrolled. Written informed consent was obtained from all patients. The patients' characteristics are listed in Supplemental Material 1. We excluded those who could not undergo CT with a urethral catheter. CT with a urethral catheter was performed in 10 patients, and PU-MRI was performed in 11 patients. Catheter insertion was difficult in one patient due to pain during insertion. This prospective clinical trial was approved by the Institutional Review Board of Hokkaido University Hospital for Clinical Research (018-0221).

2.2. Image acquisition

In this study, three gold fiducial markers (diameter, 1.5 mm) were inserted in the prostate of each patient approximately one week before the treatment-planning CT and MRI [18,19]. On the image acquisition day, treatment-planning MRI and CT were performed using the following procedures. First, the treatment-planning MRI was performed; patients were instructed by radiation technologists to urinate just before walking into the MRI room. Just a few minutes after urination, the radiation technologist started PU-MRI with the patient in supine position. The Flowchart of the image acquisition was shown in Supplemental Material 2.

We performed PU-MRI and T2-star MRI (with two slice thicknesses, 2 mm and 4 mm) using a 3.0-tesla MRI scanner with a 32-channel sensitivity-encoding (SENSE) torso cardiac coil (Achieva TX; Philips Healthcare, Best, The Netherlands). PU-MRI was performed using a non-contrast high resolution two-dimensional (2D) T2-weighted turbo spin echo (TSE) imaging sequence. The acquisition parameters for PU-MRI were as follows: resolution = 320 × 320 matrix, voxel size = 0.5 × 0.5 × 2.0 mm^3, field of view (FOV) = 160 × 160 mm^2, slices = 30, effective time echo (TE) = 80 ms, repetition time (TR) = 5093 ms, TSE factor = 9, SENSE P reduction factor = 1.4, gap = 0 mm, and acquisition direction = axial. The markers presented as signal voids in T2-weighted MRI. Also, the acquisition parameters for non-contrast 2D T2-star MRI with gradient echo imaging were as follows: resolution = 256 × 256 matrix, voxel size = 0.86 × 0.86 × 2.0 mm^3 and 0.86 × 0.86 × 4.0 mm^3 interpolated to 0.43 × 0.43 × 2.0 mm^3 and 0.43 × 0.43 × 4.0 mm^3, respectively, FOV = 220 × 220 mm^2, effective TE = 9.2 ms, TR = 1460 ms, flip angle = 20 deg, and acquisition direction = axial.

Next, the treatment-planning CT was performed using Optima CT580W (General Electronic Healthcare, Waukesha, WI) with a resolution of 512 × 512 matrix and slice thickness of 1.25 mm. We acquired two-purpose CT images. One was without a urethral catheter used for dose calculation in proton therapy. The other was with a 10-French Nelaton catheter (3.3 mm outer diameter, Sapheed®, Terumo Co., Tokyo) used to show the utility of one of the conventional visualizing methods for the prostatic urinary tract. To ensure a constant bladder volume, the CT images were taken 1 h after urination.

Finally, the data sets of all MRI and CT images with a urethral catheter were co-registered with the primary imaging CT data without a urethral catheter on Pinnacle^3 treatment planning system (TPS; ver.9.0, Philips, Inc., Madison, WI) based on the inserted fiducial markers. Fig. 1 shows sample images in axial and sagittal section; (a) treatment-planning CT for dose calculation without a urethral catheter, (b) treatment-planning CT with a urethral catheter for identification of the prostatic urinary tract, (c) T2-star MRI for target contouring, and (d) PU-MRI with TSE.

2.3. Data analysis

The prostatic urinary tract as an organ at risk (OAR) in CT with a urethral catheter and PU-MRI was contoured in a 4.0-mm diameter region of interest (ROI) including a margin of 2.0 mm to determine the planning volume of the OARs [19]. It is well-known that the accuracy and reproducibility of structures during contouring of the target organ and OARs is significantly subjected to inter-operator variability and results in uncertainty in treatment planning [20–22]. As shown in Fig. 2, the urethral ROIs were contoured by two operators (a radiation oncologist with over 10 years of experience in prostate cancer treatment planning and a medical dosimetrist with over 5 years of experience in prostate cancer treatment planning).

To investigate the inter-operator variability of the urethral ROI, we used the dice similarity coefficient (DSC_{inter}) and mean slice-wise Hausdorff distance (MSHD) [23]. A DSC_{inter} of 1 equals perfect agreement overlap, and a DSC_{inter} of 0 equals no agreement. MSHD was the average over all slices of the largest value of the smallest distance to agreement on each slice between two urethra ROIs contoured by two operators. MSHD was calculated using MIM ver. 7.0.4 (MIM Software, Inc., Cleveland, OH). We also evaluated the difference in millimeters between the inter-operator 2D displacement (d_{inter}) to the center of the urethral ROI by two operators. Similarly, we compared the 2D-discrepancies ($d_{cat-MRI}$) of the center of the urethral ROI between that on CT with a urethral catheter and that on PU-MRI in each slice, on the fusion images. The calculation formulae have been provided in Supplemental Material 3.

We calculated d_{inter} and $d_{cat-MRI}$ in the coordinates along the anterior-posterior and left–right directions. Following our previous research, the mean d_{inter} and $d_{cat-MRI}$ were calculated for the whole prostatic urinary tract and for the subgroups of the superior, middle, and inferior segments in each patient. As shown in Fig. 1, each segment of the prostatic urinary tract was defined evenly as one-third of the evenly-divided prostatic urinary tract in the clinical target volume (CTV). The superior segment was the portion on the bladder side, and the inferior segment was that on the pelvic floor side [14].

3. Results

The mean ± standard deviation (SD) volume of the prostatic urinary tract ROI was 0.61 ± 0.09 cm^3 for CT and 0.60 ± 0.08 cm^3 for PU-MRI. The mean ± SD of the DSC_{inter} value was 0.93 ± 0.04 for CT and 0.75 ± 0.05 for PU-MRI. The mean ± SD of the MSHD value was 0.17 ± 0.07 mm for CT and 0.44 ± 0.08 mm for PU-MRI.

The mean ± SD of the d_{inter} for the whole prostatic urinary tract was 0.36 ± 0.23 mm for CT and 1.00 ± 0.60 mm for PU-MRI. The mean ± SD of the d_{inter} for each segment was 0.35 ± 0.22 mm (inferior), 0.35 ± 0.21

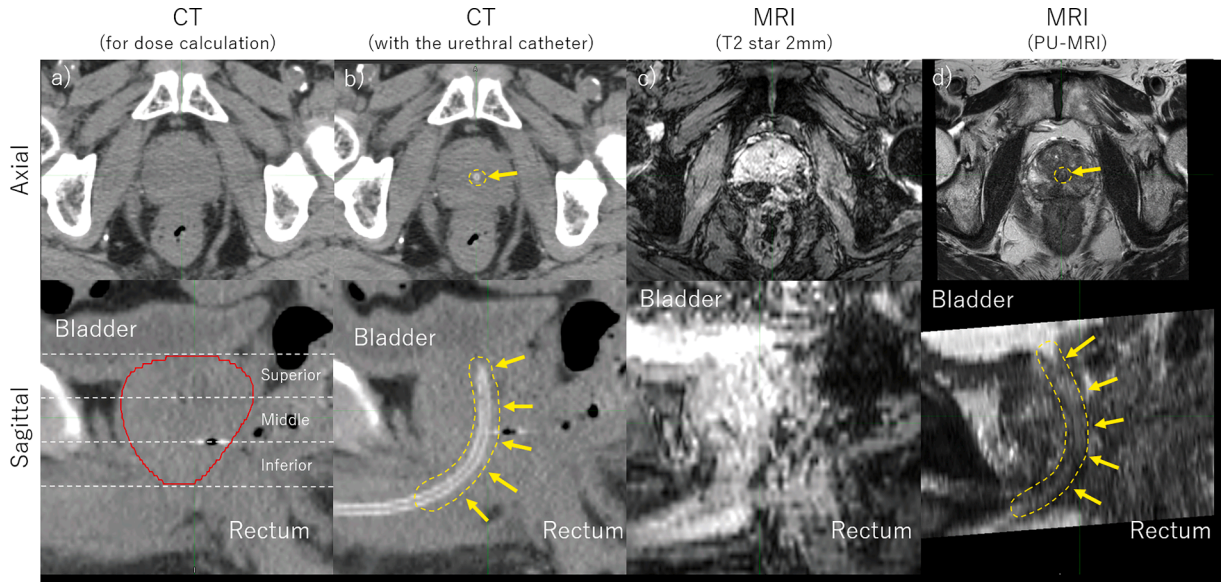

Fig. 1. Axial and sagittal images during treatment planning (Case 2). The prostatic urinary tract (yellow arrow) was identified with a urethral catheter in CT and without a urethral catheter in PU-MRI. We divided the prostatic urinary tract into three even segments in the CTV (superior, middle, and inferior). (a) Treatment-planning CT for dose calculation, (b) treatment-planning CT with a urethral catheter for visualizing the prostatic urinary tract, (c) conventional MRI without a urethral catheter for target contouring, and (d) PU-MRI with TSE. CT: computed tomography, PU-MRI: post-urination magnetic resonance imaging, TSE: turbo spin echo, CTV: clinical target volume.

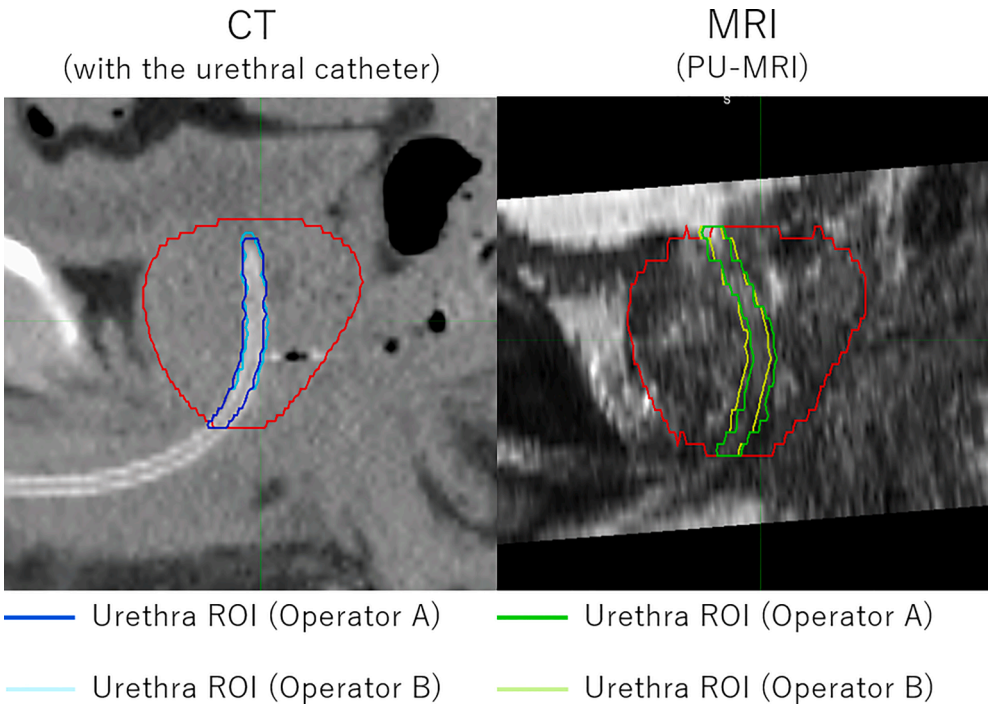

Fig. 2. Contoured urethral ROI by two operators (Case 2). The urethral ROI was identified with a urethral catheter in CT and without a urethral catheter in PU-MRI. ROI: region of interest, CT: computed tomography, PU-MRI: post-urination magnetic resonance imaging.

mm (middle), 0.38 ± 0.25 mm (superior) for CT; and 0.90 ± 0.55 mm (inferior), 1.00 ± 0.51 mm (middle), 1.11 ± 0.70 mm (superior) for PU-MRI. Also, the mean ± SD of the $d_{cat-MRI}$ for the whole prostatic urinary tract was 2.41 ± 1.14 mm for operator A and 2.22 ± 1.10 mm for operator B. The mean ± SD of the $d_{cat-MRI}$ of each segment was 2.09 ± 0.94 mm (inferior), 2.07 ± 0.90 mm (middle), 3.09 ± 1.24 mm (superior) for operator A; and 1.84 ± 0.85 mm (inferior), 2.10 ± 0.87 mm (middle), 2.77 ± 1.30 mm (superior) for operator B.

4. Discussion

In this study, we evaluated the inter-operator difference in the urethral ROI contoured by two different approaches—the prostatic urinary tract visualized through CT with a urethral catheter and PU-MRI without a urethral catheter. In our PU-MRI results that used the enhancement effect after urination, the mean values of DSC_{inter}, MSHD, and d_{inter} were 0.75, 0.44, and 1.00 mm, respectively. These results suggested that it was possible to identify the prostatic urinary tract using PU-MRI with

good accuracy.

Urethral catheter insertion is the gold standard for identifying the prostatic urinary tract in urethra-sparing radiotherapy treatment planning to reduce the risk of radiation-induced acute or late urinary toxicities [19,24]. In contrast, urethral catheter insertion is not used in patients during the irradiation of each fraction. Dekura et al. evaluated the difference between the Foley catheter and thin and soft guide-wire in the prostatic urethra, and showed that the urethral position shifted due to the insertion of the urethral catheter [14]. Although we used a thinner and softer urethral catheter, similar results were obtained. To avoid the uncertainty from the urethral catheter, an MRI scan has been acquired to identify the prostatic urinary tract [16,17]. Therefore, PU-MRI may be able to better describe the original urethral position [14].

The ultimate purpose of this study was to identify the urethra in a completely noninvasive environment using MRI with fiducial marker-based tumor-tracking radiotherapy. Since delineation of the urethra is required for urethra-sparing radiotherapy, the prostatic urinary tract was directly visualized by using a urethral catheter, Nickel-Titanium stent, or contrast agent [15,19,25]. PU-MRI sequence without these uncertainty factors indicated the potential for urethra contouring with a small error between observers, which would be beneficial to the patients. However, this study has potential limitations, such as the low number of patients and the inter-observer variability in urethral contouring. Although further accurate contouring to estimate the intra- and inter-operator variabilities is required in a larger number of patients, our proposed method will be useful for identifying the prostatic urinary tract without the use of a urethral catheter.

In conclusion, we proposed a method using post-urination high resolution T2-weighted 3.0 T MRI in urethra-sparing treatment planning for localized prostate cancer. Our results demonstrated that the inter-operator prostatic urinary tract ROI matched with a high accuracy, not only in CT with a urethral catheter, but also in PU-MRI. Thus, in the treatment planning for localized prostate cancer, PU-MRI is useful in identifying the urethra non-invasively, without using a urethral catheter.

Declaration of Competing Interest

The authors declare the following financial interests/personal relationships which may be considered as potential competing interests: Dr. Shimizu reports grants from Hitachi Ltd, during the conduct of the study; In addition, Dr. Shimizu has a patent Charged particle beam system, US 14/524,495 licensed, and a patent Radiotherapy control apparatus and radiotherapy control program, US9616249 licensed. Other authors have no relevant conflicts of interest to disclose.

Acknowledgement

We are grateful to the therapists and nurses at the Proton Beam Therapy Center, Hokkaido University Hospital, Sapporo, Japan.

Role of the funding source

This research was supported by Japan Society for the Promotion of Science (JSPS), Japan KAKENHI (Grant Numbers: JP18K15577 and JP18H02758), and Japan Agency for Medical Research and Development (AMED), Japan (Grant Number: JP18he1602004).

Appendix A. Supplementary data

Supplementary data to this article can be found online at https://doi.org/10.1016/j.phro.2021.03.002.

References

[1] Fischer-Valuck BW, Rao YJ, Michalski JM. Intensity-modulated radiotherapy for prostate cancer. Transl Androl Urol 2018;7:297–307.
[2] Georg D, Hopfgartner J, Gòra J, Kuess P, Kragl G, Berger D, et al. Dosimetric considerations to determine the optimal technique for localized prostate cancer among external photon, proton, or carbon-ion therapy and high-dose-rate or low-dose-rate brachytherapy. Int J Radiat Oncol Biol Phys 2014;88:715–22.
[3] Zelefsky MJI, Levin EJ, Hunt M, Yamada Y, Shippy AM, Jackson A, et al. Incidence of late rectal and urinary toxicities after three-dimensional conformal radiotherapy and intensity-modulated radiotherapy for localized prostate cancer. Int J Radiat Oncol Biol Phys 2008;70:1124–9.
[4] Beckendorf V, Guerif S, Le Prise E, Cosset JM, Bougnoux A, Chauvet B, et al. 70 Gy versus 80 Gy in localized prostate cancer: 5-year results of GETUG 06 randomized trial. Int J Radiat Oncol Biol Phys 2011;80:1056–63.
[5] Rana Z, Cyr RA, Chen LN, Kim BS, Moures RA, Yung TM, et al. Improved irritative voiding symptoms 3 years after stereotactic body radiation therapy for prostate cancer. Front Oncol 2014;4:290.
[6] Arscott WT, Chen LN, Wilson N, Bhagat A, Kim JS, Moures RA, et al. Obstructive voiding symptoms following stereotactic body radiation therapy for prostate cancer. Radiat Oncol 2014;9:163.
[7] Janowski EM, Kole TP, Chen LN, Kim JS, Yung TM, Collins BT, et al. Dysuria following stereotactic body radiation therapy for prostate cancer. Front Oncol 2015;5:151.
[8] Sanda MG, Dunn RL, Michalski J, Sandler HM, Northouse L, Hembroff L, et al. Quality of life and satisfaction with outcome among prostate-cancer survivors. New Engl J Med 2008;358:1250–61.
[9] Villeirs GM, De Meerleer GO. Magnetic resonance imaging (MRI) anatomy of the prostate and application of MRI in radiotherapy planning. Eur J Radiol 2007;63:361–8.
[10] Dirix P, Haustermans K, Vandecaveye V. The value of magnetic resonance imaging for radiotherapy planning. Semin Radiat Oncol 2014;24:151–9.
[11] Murray LJ, Lilley J, Thompson CM, Cosgrove V, Mason J, Sykes J, et al. Prostate stereotactic ablative radiation therapy using volumetric modulated arc therapy to dominant intraprostatic lesions. Int J Radiat Oncol Biol Phys 2014;89:406–15.
[12] Repka MC, Guleria S, Cyr RA, Yung TM, Koneru H, Chen LN, et al. Acute urinary morbidity following stereotactic body radiation therapy for prostate cancer with prophylactic alpha-adrenergic antagonist and urethral dose reduction. Front Oncol 2016;6:122.
[13] Gardner A, Mitchell B, Beckingham W, Fasugba O. A point prevalence cross-sectional study of healthcare-associated urinary tract infections in six Australian hospitals. BMJ Open 2014;4:e005099.
[14] Dekura Y, Nishioka K, Hashimoto T, Miyamoto N, Suzuki R, Yoshimura T, et al. The urethral position may shift due to urethral catheter placement in the treatment planning for prostate radiation therapy. Radiat Oncol 2019;14:226.
[15] Kataria T, Gupta D, Goyal S, Bisht SS, Chaudhary R, Narang K, et al. Simple diagrammatic method to delineate male urethra in prostate cancer radiotherapy: an MRI based approach. Br J Radiol 2016;89:20160348.
[16] Zakian KL, Wibmer A, Vargas HA, Alberts E, Kadbi M, Mychalczak B, et al. Comparison of motion-insensitive T2-Weighted MRI pulse sequences for visualization of the prostatic urethra during MR simulation. Practical Radiat Oncol 2019;9:e534–40.
[17] Rai R, Sidhom M, Lim K, Ohanessian L, Liney GP. MRI micturating urethrography for improved urethral delineation in prostate radiotherapy planning: a case study. Phys Med Biol 2017;62:3003–10.
[18] Shimizu S, Shirato H, Kitamura K, Shinohara N, Harabayashi T, Tsukamoto T, et al. Use of an implanted marker and real-time tracking of the marker for the positioning of prostate and bladder cancers. Int J Radiat Oncol Biol Phys 2000;48:1591–7.
[19] Shimizu S, Nishioka K, Suzuki R, Shinohara N, Maruyama S, Abe T, et al. Early results of urethral dose reduction and small safety margin in intensity-modulated radiation therapy (IMRT) for localized prostate cancer using a real-time tumor-tracking radiotherapy (RTRT) system. Radiat Oncol 2014;9:1–8.
[20] Lawton CA, Michalski J, El-Naqa I, Buyyounouski MK, Lee WR, Menard C, et al. RTOG GU radiation oncology specialists reach consensus on pelvic lymph node volumes for high-risk prostate cancer. Int J Radiat Oncol Biol Phys 2009;74:383–7.
[21] Batumalai V, Koh ES, Delaney GP, Holloway LC, Jameson MG, Papadatos G, et al. Interobserver variability in clinical target volume delineation in tangential breast irradiation: a comparison between radiation oncologists and radiation therapists. Clin Oncol (R Coll Radiol) 2011;23:108–13.
[22] Velker VM, Rodrigues GB, Dinniwell R, Hwee J, Louie AV. Creation of RTOG compliant patient CT-atlases for automated atlas based contouring of local regional breast and high-risk prostate cancers. Radiat Oncol 2013;8:1–8.
[23] Dice LR. Measures of the amount of ecologic association between species. Ecology 1945;26:297–302.
[24] Dubouloz A, Rouzaud M, Tsvang L, Verbakel W, Björkqvist M, Linthout N, et al. Urethra-sparing stereotactic body radiotherapy for prostate cancer: how much can the rectal wall dose be reduced with or without an endorectal balloon? Radiat Oncol 2018;13:114.
[25] Thomsen JB, Arp DT, Carl J. Urethra sparing – potential of combined Nickel–Titanium stent and intensity modulated radiation therapy in prostate cancer. Radiother Oncol 2012;103:256–60.